



Physical and Structural Properties of Porous Kaolin/Co-Ferrite for Water Treatment

¹Wasan Ziedan*, ²Mukhlis M. Ismail, ²Wafaa A. Hussain

¹State Company for Construction Industries, Ministry of Industry and Minerals – Iraq

²Department of Applied Sciences, University of Technology – Iraq

Article information

Article history:

Received: September, 02, 2023

Accepted: January, 26, 2024

Available online: March, 10, 2024

Keywords:

Cobalt ferrite,

XRD,

FT-IR,

FE-SEM,

Kaolin

*Corresponding Author:

Wasan Ziedan

as.21.49@grad.uotechnology.edu.iq

Abstract

Aqueous solutions with heavy metals such as Cr (VI), Pb, and Cd (II) can have an adverse effect on human health because of their toxicity. As a result, it is important to remove these heavy metals from the aquatic environment to save the human healthy. X-ray diffraction (XRD), Fourier-transform infrared spectroscopy (FTIR), and field-emission scanning electron microscopy (FE-SEM) used in this research to characterize cobalt ferrite (CoFe_2O_4) nanoparticles and confirm the structure of $\text{Co-Fe}_2\text{O}_4$. These particles were used to make porous samples and burned at 1050 °C in mixtures of (0, 3, 5, 7, and 10) wt.% of cobalt ferrite and kaolin with 20 wt.% of charcoal. These samples serve as adsorbents that remove Pb from the wastewater. The highest rates of removal were confirmed using various treatments at (pH 3, 7, and 9). A Williamson-Hall plot was used to determine the crystal size (33) nm. The FT-IR spectra exhibited spinel-ferrite characteristics. Studies using FE-SEM demonstrated that the sample was in Nano crystalline. Using a vibrating sample magnetometer (VSM), different magnetic properties are taken from the hysteresis loops such as saturation magnetization (M_s) and remanence (M_r) and coercivity (H_c). It was found that increasing ferrite content, increased adsorption efficiency.

DOI: [10.53293/jasn.2024.7103.1245](https://doi.org/10.53293/jasn.2024.7103.1245), Department of Applied Sciences, University of Technology - Iraq.

© 2024 The Author(s). This is an open access article under the CC BY 4.0 License.

1. Introduction

The treatment of wastewater is a crucial step in getting polluted water back into the environment. Wastewater is created in large quantities as the world's population grows. Organic and inorganic pollutants, and hazardous heavy metals like CO, Pb, Hg and Cd, are among the many contaminants found in wastewater [1]. Even at very low concentrations, lead (Pb) is one of the most hazardous pollutants [2]. Various methods of wastewater treatment have been developed and used. Some of these techniques include centrifugation, filtration, flotation, distillation, ion exchange, adsorption, microfiltration and ultrafiltration. Adsorption is a widely used process to remove contaminants from liquids. Adsorption has proven to be a versatile isolation method for solute separation [3]. The adsorption process forms a layer of adsorbate (metal ions) on the surface of adsorbents. Adsorption onto a solid adsorbent includes three major steps: transportation of the pollutant to the adsorbent surface from aqueous solution, adsorption onto the solid surface, and transport within the adsorbent particle. Generally, electrostatic attraction

causes charged pollutants to adsorb on differently charged adsorbents because heavy metals have a vigorous affinity for hydroxyl (OH^-) or other functional group surfaces [4]. Because of the interaction for metal ions with sorbents, many studies show that nanoparticles are efficient sorbents for the removal of heavy metal ions [5-12].

Porous ceramics have been extensively used as building materials and for thermal insulation. In the field of environmental sciences, advanced applications such as filters, catalytic supports, and membranes are expanding quickly [13]. One of the most common natural clays is kaolin, which may be found in rocks and soils all around the world. Because kaolin has a constant negative surface charge, it is effective at adsorbing heavy metals. Heavy metal transport and distribution in soil and water are regulated by kaolin [14]. When kaolin is fired, it undergoes a phase transformation and converts to mullite. Mullite is a refractory ceramic material that has excellent high-temperature properties, including improved thermal shock and thermal stress resistance, low thermal expansion, good strength. Mullite is used in a variety of applications, including as a refractory material, adsorbent, and catalyst support [15]. Due to their potential use in magnetic fluids, high-density magnetic recording, and other applications, magnetic nanoparticles have been the topic of extensive investigation. Cobalt ferrite (CoFe_2O_4) is one of several magnetic materials that has undergone extensive research [16]. They are utilized in numerous technological applications, such as high-quality filters, transformer cores, and inductors [17]. Numerous techniques, including chemical reactions, sol-gel, microwave plasma, host template, co-precipitation, microemulsion, and chemical vapor deposition, have been devised for the manufacture of nanoferrites [18, 19]. The sol-gel approach is a simple and effective one [20]. In order to generate porous samples made by the slip casting process to remove Pb ion from wastewater, the primary purpose of this study was to study the effectiveness of employing kaolin, charcoal as pore formers with cobalt ferrite nanoparticles. Utilizing XRD, FESEM, and VSM, ferrite nanoparticles made using the sol-gel technique were characterized.

2. Experimental Procedure

2.1. Synthesis of $\text{Co-Fe}_2\text{O}_4$

Cobalt ferrite powder was synthesized using sol-gel auto combustion method by dissolving cobalt nitrate $\text{Co}(\text{NO}_3)_2 \cdot 6\text{H}_2\text{O}$, iron nitrate $\text{Fe}(\text{NO}_3)_3 \cdot 9\text{H}_2\text{O}$ and citric acid $\text{C}_6\text{H}_8\text{O}_7$, were from (CDH/India), in deionized water. The molar ratio of cobalt and ferric nitrates $\text{Fe}(\text{NO}_3)_3 \cdot 9\text{H}_2\text{O}$ to citric acid ratio was 1:2:3. The solution pH was adjusted to be at (7) using ammonia hydroxide NH_4OH that was added in the form of drops with continuous mixing by magnetic stirrer. The additional water was removed by heating at (60-80) °C with continue stirring. The solution was converted into a gel till all gel was completely burnt out to form a fluffy loose structure (ash), which was ground well in a mortar to get Cobalt ferrite nanoparticles.

Fig. 1 a, depicts the green body of samples that contain kaolin powder. A chemical analysis of Iraqi kaolin, which was locally discovered in the western desert (Dwekhla), was conducted to determine the composition and percentages of oxides to demonstrate its suitability for research, as shown in Table (1) [21]. It is clear from the table using XRF that kaolin contains good proportions of silicon oxide (silica) and aluminum oxide (alumina). Kaolin in a 20% ratio with wood charcoal, as well as the various weight percentages (0, 3, 5, 7, and 10) wt. % of cobalt ferrite that were used to create the porous samples. The samples were then made using the slip-casting method, with dimension (30 mm * 5 mm) that were dried at 100 °C, then sintered at 1050 °C for two hours, getting samples as shown in Fig. 1 b.

Charcoal was utilized in this work to create a pore. It was crushed and a milling method offered by (ball mill) that used to generate fine particle sizes. Then, the sieving process was carried out by using a sieve shaker to yield particle size 25 μm .

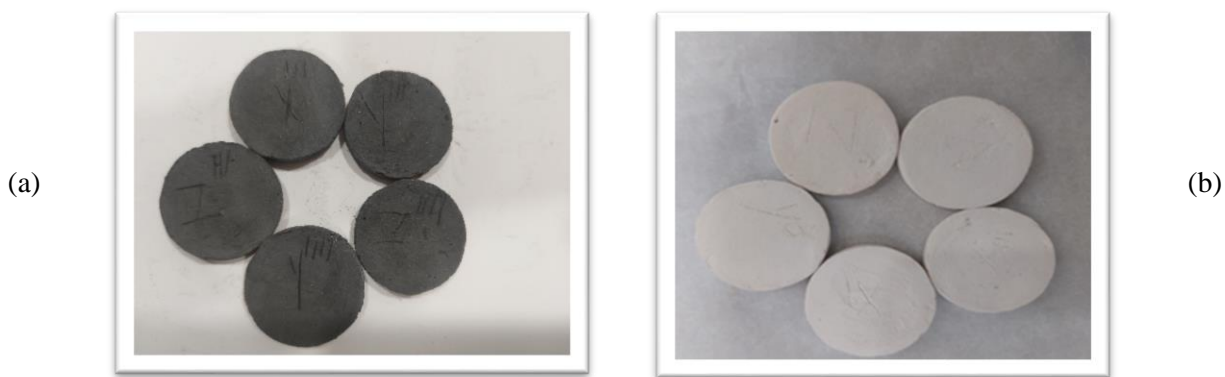


Figure 1: (a) Green body of porous ceramics, (b) porous sintered ceramics.

Table 1. Chemical Composition for kaolin.

Oxides	SiO ₂	Al ₂ O ₃	Fe ₂ O ₃	CaO	TiO ₂	K ₂ O	Na ₂ O	MgO	loss on ignition%
wt. %	49.38	32.72	2.07	1.19	1.08	0.44	0.22	0.18	12.42

2.2. Characterizations

Fourier transform infrared were describe the formation of the spinel structure in the 400–4000 cm⁻¹ range. In order to investigate the cobalt-ferrite nanoparticles, an XRD machine (Shimadzu 6000, made in Japan) with Cu and Ka radiation in the 2° to 90° ($\lambda = 0.15406$ nm) range. Field emission scanning electron microscope (FE-SEM) (Inspect f50 FEI company- Holland) at high magnifications, describe the morphology of particles. In order to analyze the elemental components of particles, the Energy-dispersive X-ray spectroscopy (EDS) (Axia chemi-Thermo scientific company-Holland) were analyzed.

2.3. Magnetic Characterization

The properties of magnetic nanoparticles were measured by vibrating specimen magnetometer (VSM), which was utilized to build a hysteresis loop with a magnetic field that cycled between (-10,000 G to 10,000 G) at room temperature. Hysteresis loops are used to measure saturation magnetization (MS), coercivity (Hc), and remanent magnetization (Mr).

2.4 Mechanical Properties

The sample is placed vertically below the piston of a hydraulic press, which measures diametrical strength. In accordance with (ASTM-C773), the diametrical strength computed using equation (1), [21, 22].

$$\sigma = \frac{2F}{\pi DT} \quad (1)$$

Where: (σ) flexural strength (Pa), F load at the fracture point (N), D specimen diameter (mm), T specimen thickness (mm).

2.5. Adsorption of Metals Ions and Removal Efficiency

By using an adsorption technique, porous Kaolinite/CO-Ferrite samples removed Pb ions. The adsorption process, which involves the development of physical or chemical bonding for porous samples, allows for flexibility in both design and operation [23]. The removal rate (η) was calculated using equation (2), [24]:

$$\eta = \frac{C_0 - C_e}{C_0} \times 100\% \quad (2)$$

Where: C₀, C_e are the initial and the final concentrations of Pb (II) ion (mg/l), respectively.

2.6. Effect of pH

Discover the effects of pH on Pb adsorption using porous Kaolin/Co-Ferrite samples. In a funnel, as illustrated in Fig. 2, a fixed porous sample of each combination received 100 mL of a 250 ppm Pb solution. Using NaOH or HCl, the pH (3, 7 and 9) of the solution was changed to the appropriate value. Finally, an atomic adsorption spectrophotometer (AAS) type (AA-7000-SHIMADZU) was used to determine the collected solution.

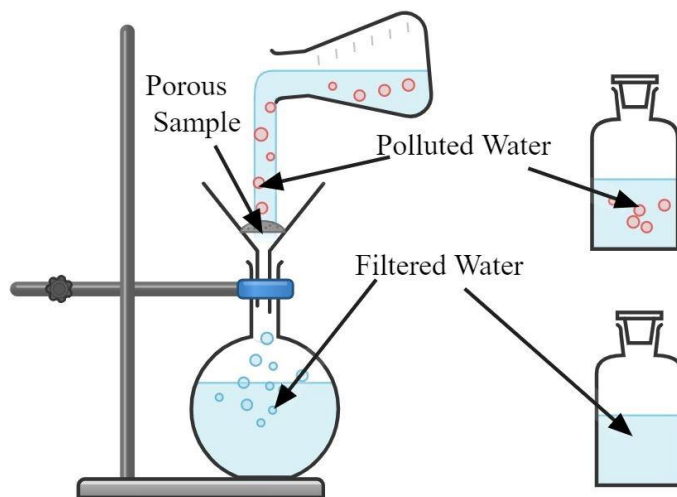


Figure 2: Adsorption process used in water treatment; heavy metals (Pb) ions in the water are represented in red on the surface of the nanoporous adsorbents.

3. Results and Discussion

3.1 Analyzed Structure

FT-IR spectra of Co-Fe₂O₄ powder are shown in Fig. 3, taken at room temperature. Absorption peak at 570.93 cm⁻¹ corresponding to intrinsic stretching vibrations of metal at the tetrahedral site, whereas the lowest band, observed at 422.41 cm⁻¹, is due to the octahedral–metal stretching. Co²⁺ ions usually occupy octahedral-site, while Fe³⁺ ions has the tendency to occupy both octahedral and tetrahedral sites [25].

The peaks around 950.91 cm⁻¹ are belong to the Fe–Co alloy system. The band at 1381.03 cm⁻¹ is ascribed to the symmetric vibration of the NO₃⁻ group. The peak at 1585.49 cm⁻¹ were assigned to stretching and bending vibrations of absorption water on surfaces of nanostructures. The peaks at 2856.58, 2922.16 cm⁻¹ are due to C–H stretching, and O–H stretching respectively [26]. The vibrational frequencies associated with cobalt ferrite material centered at 3130.47 cm⁻¹ are due to O–H stretching vibrations [27].

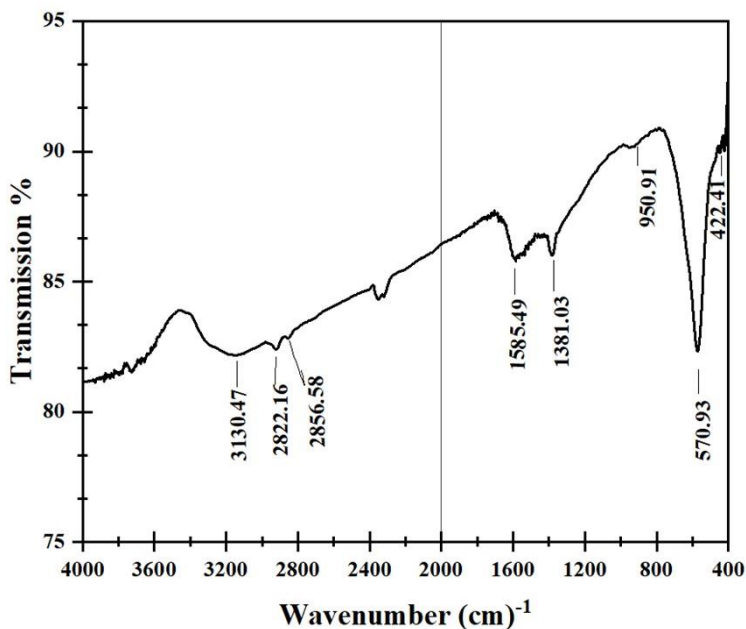


Figure 3: FT-IR spectra of Cobalt Ferrite.

XRD pattern of $\text{Co-Fe}_2\text{O}_4$ nanoparticles are depicted in Fig. 4, the diffraction peak at 30.3° , 35.6° , 43.14° , 53.72° , 57.14° , 62.74° is recognized to the miller indices which are: (220), (311), (400), (422), (511) and (440), respectively. The most intense peak and the preferred orientation was observed at (311) with crystallite size to be (33) nm. No other peaks are present, indicating that the single-phase spinel structure of the synthesized samples matches JCPDS-ICDD file number 22-1086 [28].

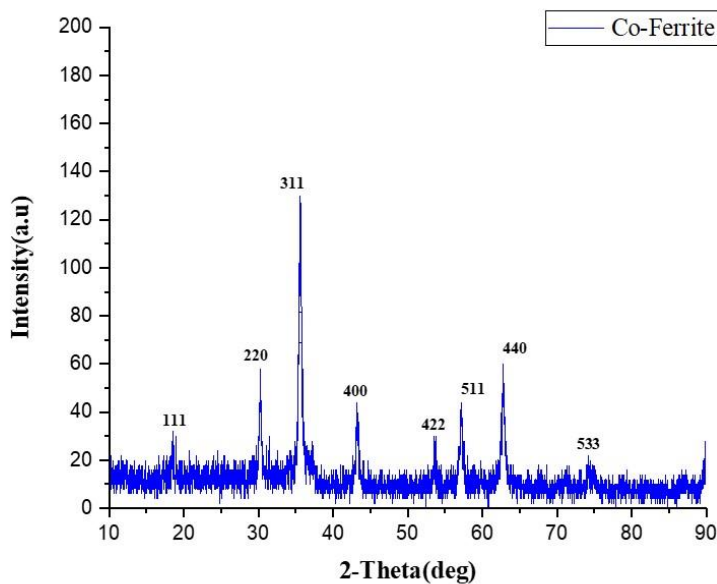


Figure 4: XRD Pattern of $\text{Co-Fe}_2\text{O}_4$.

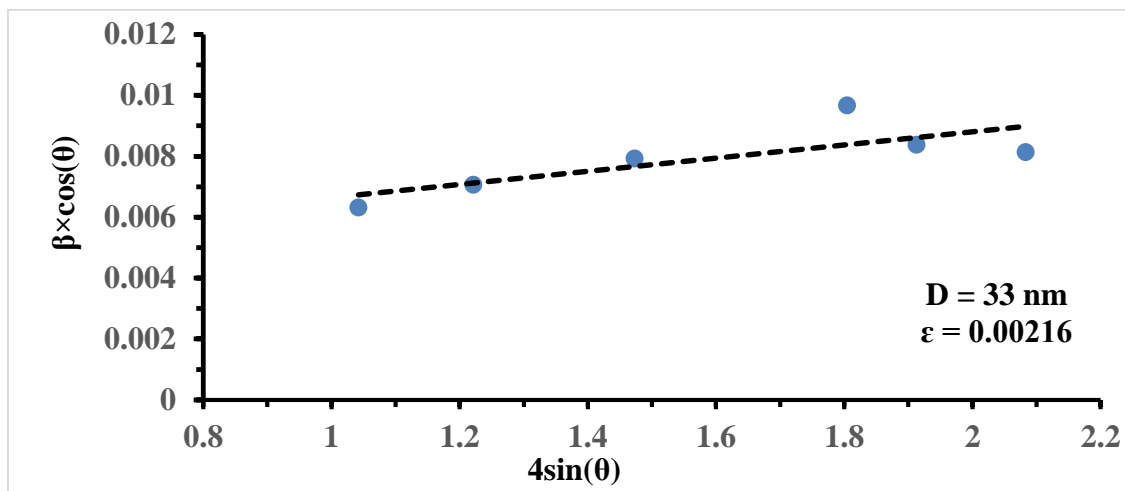


Figure 5: W-H plot of Co-Fe₂O₄.

The crystallite size (D) and lattice strain (ϵ) were acquired through Williamson -Hall plot [29], as shown in the Fig.5, the crystallite size was 33 nm while the strain was 0.00216.

The FE-SEM examination of CoFe₂O₄ nanoparticles produced using the sol-gel process is seen in Fig. 6, shows that the substance is made up of nanoparticles with a form that is very close to spherical. An attached energy dispersive spectrometer (EDS) was used to investigate the qualitative chemical composition of cobalt ferrite which was made to accurately indicate and confirm the presence of Co, Fe and O present in the composition. The energy dispersion spectrum shows that approximately the same amount of elements are present in the chemical structure without any significant impurities.

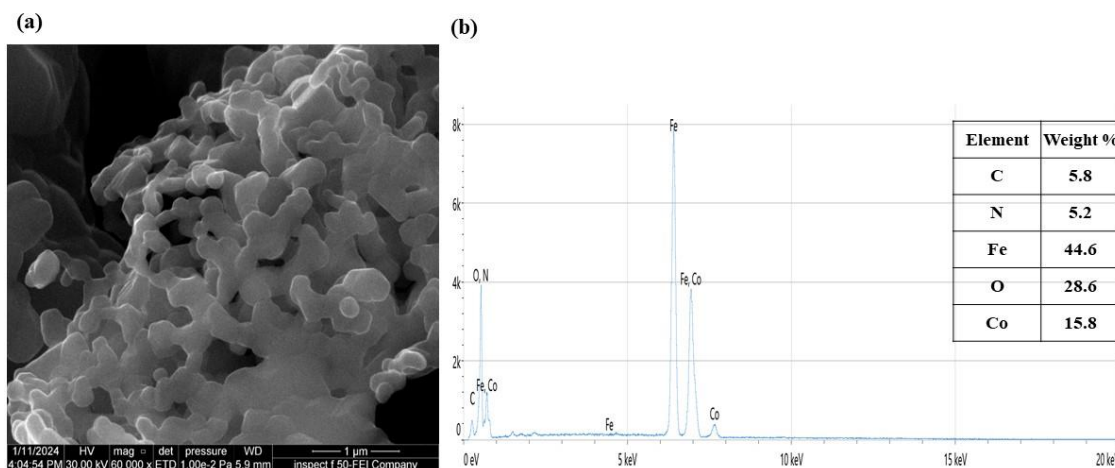


Figure 6: FE-SEM micrographs of (a) Co-ferrite, and (b) the EDS technique for Co-ferrite.

The FE-SEM observation of kaolin fired at 1050 °C Fig. 7 shows a microstructure with mullite crystals. They are originated from kaolinite decomposition by firing present in the sample. It can be observed in detail needle shape of small sizes of mullite crystals.

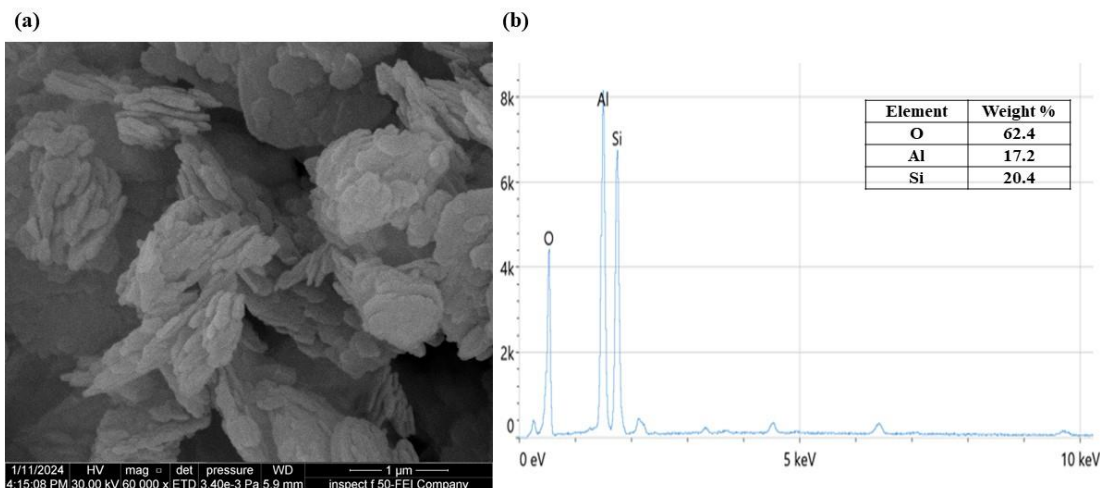


Figure 7: FE-SEM micrographs: (a) of mullite phase obtained after firing of kaolinite clay at 1050 °C, (b) EDS analysis of the obtained mullite.

FE-SEM for charcoal fired at 1050 °C shown in Fig. 8, it can be seen that charcoal presents a filamentous morphology with an axial stripe arrangement, and that some longitudinal grooves and many irregular particles are distributed on the surface. More holes and craters are observed. EDS of charcoal fired at 1050 °C observation it was contain high levels of C and O elements, which occupy a large percentage, were charcoal-forming elements, while the other elements were coal impurities. The results shown in the figure indicate that Al, Si, K, Ca, Mg and Fe were present in relatively small numbers.

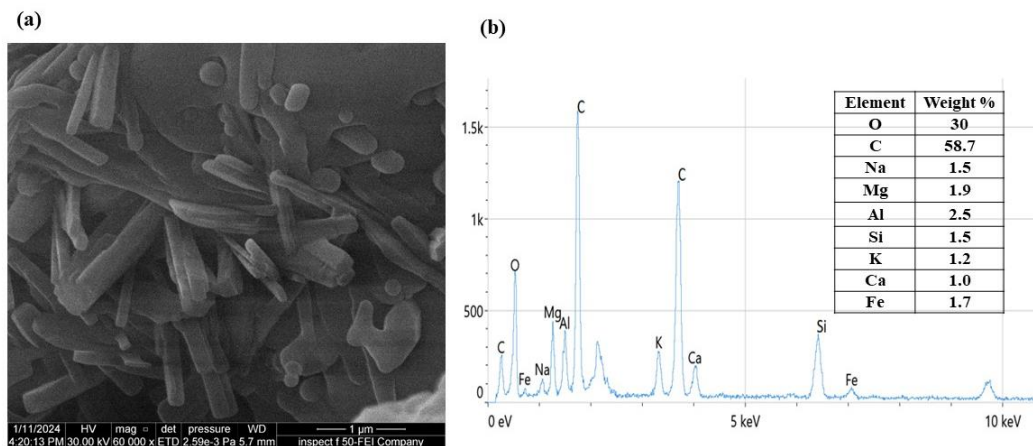


Figure 8: FE-SEM micrographs: (a) of charcoal fired at 1050 °C, (b) EDS analysis of charcoal.

3.2 Magnetic Measurements

Fig. 9 represents magnetic hysteresis (M–H) loops of cobalt ferrite nanoparticle, the hysteresis loop curve of the nanoparticles indicated hard magnetic material [30, 31]. Saturation magnetization, remnant magnetization, the coercivity, Squareness ratio M_r/M_s of CoFe_2O_4 nanoparticles obtained from hysteresis loop are found to be 48.85 emu/g, 23.68 emu/g, 2000 Oe, 0.48 respectively. In the hysteresis curve of CoFe_2O_4 nanoparticles prepared with sol-gel method. The calculated saturation magnetization (M_s) value of CoFe_2O_4 nanoparticles was obtained as 48.85 emu/g, which is lower than the value reported for bulk samples (80 emu/g) [32], which is a result of the superparamagnetic nature of the magnetic nanoparticles [2].

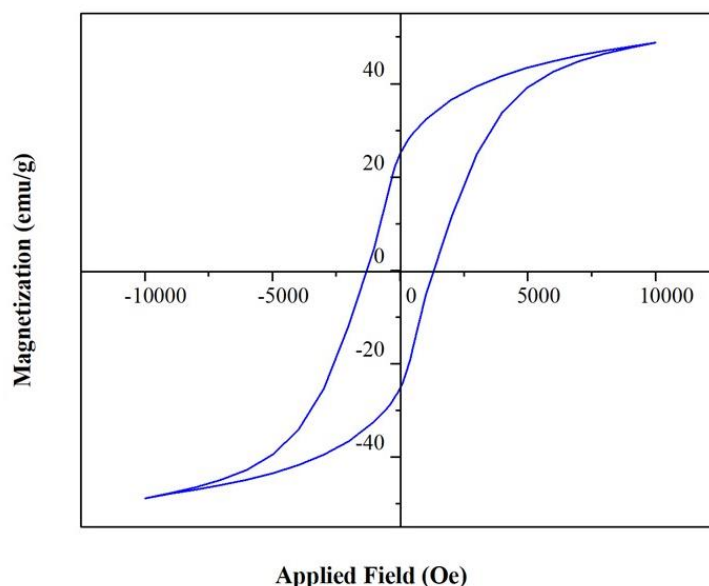


Figure 9: Hysteresis curve of Co-Ferrite.

3.3 Mechanical Properties (Diametrical Compressive Strength):

Adding of (5) wt. % of CoFe_2O_4 nanoparticles increases compressive strength of the ceramic filter, as seen in Fig. 10, this may be attributed to decreased porosity with increased ferrite percentages, which increase the specimens' strength to the load imposed on it.

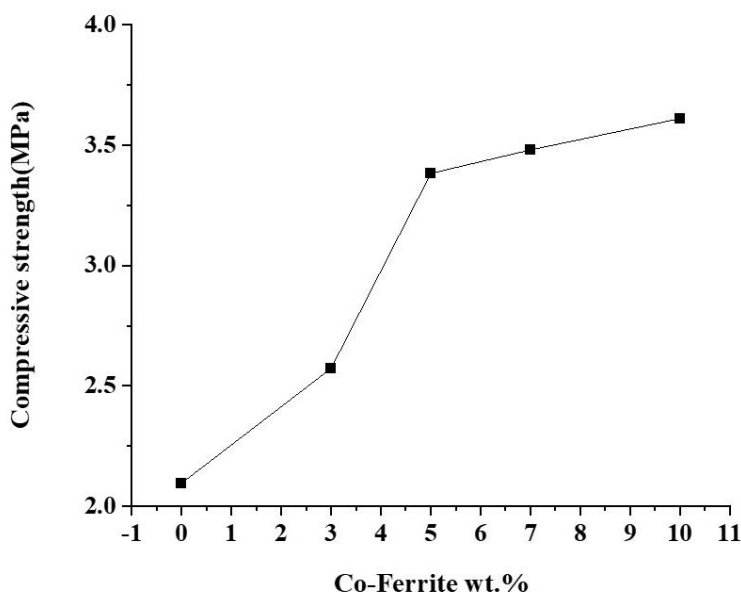


Figure 10: Compressive strength of Kaolin and charcoal with different ratio of Co-Ferrite (0.3.5.7.10) %.

3.4 Adsorption of Heavy Metal Ion (Effect of pH):

As shown in Fig. 11, the influence of pH on the Pb adsorption efficiency was examined at pH levels of (3, 7), and (9). The results showed that the pH of the solution had an impact on the adsorption of Pb. At pH 3, shown that all ferrite-based samples in this investigation take up Pb with greater efficiency. Adsorption just lowers at pH 7 and reaches its lowest removal effectiveness at pH 9. This result, which is known to be true for metal ions like Pb that have a significant tendency to undergo hydrolysis [2,32], demonstrates that at 10% cobalt ferrite in all examined pH values, Pb was absorbable with maximum efficiency. The lowest proportion of ferrite was introduced at pH 9, which also yielded the lowest adsorption effectiveness for all samples.

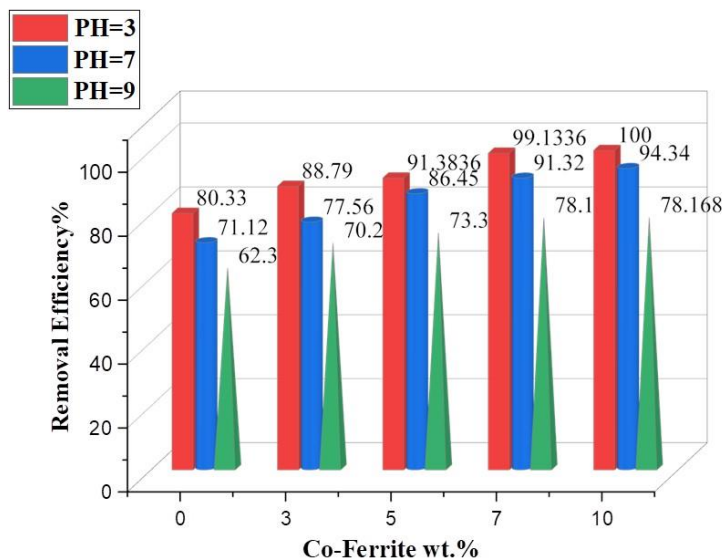


Figure 11: Effect of pH on removal efficiency of pd, using Kaolin and charcoal with different ratio of Co-Ferrite (0.3.5.7.10) %.

4. Conclusions

In this study aimed to synthesize porous CoFe_2O_4 /Kaolin via slip casting method that optimum removal efficiencies for Pb ions were obtained to be 100% at pH 3, it has been shown that the amount of magnetic materials added at the highest percentage gave the best results in removing heavy metals from polluted water. The characterization results confirmed XRD the single spinel structure with a crystal size of 33 nm. The bands of metal oxide were mentioned by FT-IR confirmed the formation of spinel ferrite. The VSM techniques confirmed the magnetic property of CoFe_2O_4 , indicated hard magnetic material.

Conflict of Interest

The authors declare that they have no conflict of interest.

References

- [1] R. Ramadan, "Physical study of cobalt ferrite and its application in purification of water," *Applied Physics A*, vol. 125, no. 12, p. 825, 2019.
- [2] D. A. Tessema and D. D. Alemayehu, "A comparative study on Pb^{2+} removal efficiencies of fired clay soils of different particle size distributions," *African Journal of Environmental Science and Technology*, vol. 7, p. 824–832, 2013.
- [3] A. Cescon and J.Q. Jiang, "Filtration Process and Alternative Filter Media Material in Water Treatment," *Water*, vol. 12, p. 3377, 2020.
- [4] Z. Raji, A. Karim, A. Karam, and S. Khalloufi, "Adsorption of Heavy Metals: Mechanisms, Kinetics, and Applications of Various Adsorbents in Wastewater Remediation—A Review," vol. 1, p. 775–805, 2023.
- [5] H. S. Al- Lami, M. A. Saadallah, and W. A. Hussain, "Using non-Ferrous metals in processing of porous ceramics," *Eng. of Technology*, vol. 21, p. 17-28, 2002.
- [6] W. A. Hussain and H. S. Al- Lami, "Effect of Forming Methods on the Properties of Controlled Porous Ceramics," *Eng. of Technology*, vol.26, p. 16-28, 2008.
- [7] M. M. Ismail, W. A. Hussain, and F. S. Hashim, "Bio-Application of Poly (Vinyl Alcohol)/Biphasic Calcium Phosphate Scaffold as Bone Tissue Replacement," *Current Materials Science*, vol. 15, p. 271–279, 2022.
- [8] F. Hashim, M. M. Ismail, and W. Hussain, "Tri-calcium Phosphate (Nanoparticles/Nanofibers)/PVA for Bone Tissue Engineering," *Acta Physica Polonica A*, vol. 140, p. 337–343, 2021.

- [9] W. A. Hussain, M. M. Ismail, and S. Taher, "Incorporation of Treated Woven Carbon Fiber to Methacrylate Resin for Heat-Cured Acrylic Denture Composite," *Journal of Biomimetics, Biomaterials and Biomedical Engineering*, vol. 56, p. 153–164, 2022.
- [10] W.A.Hussain and L.H. Alwan, "Preparation of Calcium Phosphate via Precipitation Technique," *Eng. of Technology*, vol.33, p. 1412-1419, 2015.
- [11] T.Y. Taher and W.A. Hussain, "The effect of acidic treatment of carbon fiber on denture mechanical properties," *Journal of Physics: Conference Series*, vol 1879, p. 032082, 2021.
- [12] R. Q. Nafil and M. S. Majeed, "Frequency doubling by nonlinearity of TiO₂ nanomaterial, " *Heliyon*, vol. 6, p. e03649, 2020.
- [13] W. A. Khoso, N. Haleem, M. A. Baig, and Y. Jamal, "Synthesis, characterization and heavy metal removal efficiency of nickel ferrite nanoparticles (NFN's)," *Scientific Reports*, vol. 11, p. 3790, 2021.
- [14] Z.H. Wen, Y.S. Han, L. Liang, and J.B. Li, "Preparation of porous ceramics with controllable pore sizes in an easy and low-cost way," *Materials Characterization*, vol. 59, p. 1335–1338, 2008.
- [15] Y. Zhang, Z. Wei, M. Li, X. Wu, and W. Wang, "Preparation and Modification of Mullite Whiskers/Cordierite Porous Ceramics for Cu²⁺ Adsorption and Removing," *ACS Omega*, vol. 5, p. 15691–15701, 2020.
- [16] J. Liu, X. Wu, Y. Hu, C. Dai, Q. Peng, and D. Liang, "Effects of Cu(II) on the Adsorption Behaviors of Cr(III) and Cr(VI) onto Kaolin," *Journal of Chemistry*, vol. 2016, p. e3069754, 2016.
- [17] Y.C. Mattei, O. P. Perez, M.S.Tomar, and F. Roman, "Optimization of Magnetic Properties in Cobalt Ferrite Nanocrystals," *In ENS*, vol. 2007, p. 63-67, 2007.
- [18] S.S.Shinde, "Crystal Structure and Magnetic Interactions of Ferrites," *International Journal of Science and Research*, vol. 5, p. 2319-7064, 2015.
- [19] Z. Yue, W. Guo, J. Zhou, Z. Gui, and L. Li, "Synthesis of nanocrystalline ferrites by sol–gel combustion process: the influence of pH value of solution, " vol. 270, p. 216–223, 2004.
- [20] D. Bokov, A.T. Jalil, S. Chupradit, W. Suksatan, M.J. Ansari, I.H. Shewael, *et al.*, "Nanomaterial by Sol-Gel Method: Synthesis and Application," *Advances in Materials Science and Engineering*, vol. 2021, p. 1–21, 2021.
- [21] H. Jabbar, E. Muhi, and T. Hussien, "Purifications of Iraqi Petroleum Using Ceramic Ball Nano Cobalt Nickel Ferrite Filter," *Karbala international journal of modern science*, vol. 8, p. 514–521, 2022.
- [22] M. Patel, S. Mishra, R. Verma, and D. Shikha, "Synthesis of ZnO and CuO nanoparticles via Sol gel method and its characterization by using various technique, " *Discover Materials*, vol. 2, p. 1, 2022.
- [23] R. Pemberton, J. Summerscales and J. Graham-Jones, "Marine Composites: Design and Performance," Woodhead Publishing imprint, Cambridge, 2019.
- [24] C. Liosis, A. Papadopoulou, E. Karvelas, T. E. Karakasidis, and I. E. Sarris, "Heavy Metal Adsorption Using Magnetic Nanoparticles for Water Purification: A Critical Review, " *Materials*, vol. 14, p. 7500, 2021.
- [25] A. Yakubu, Z. Abbas, N. Ibrahim, and M. Hashim, "Effect of Temperature on Structural, Magnetic and Dielectric Properties of Cobalt Ferrite Nanoparticles Prepared via Co-precipitation Method," *Physical Science International Journal*, vol. 8, p. 1–8, 2015.
- [26] R. Lakshmanan, "Application of magnetic nanoparticles and reactive filter materials for wastewater treatment," 2013.
- [27] S. Yavari, N.M. Mahmodi, P. Teymouri, B. Shahmoradi, and A. Maleki, "Cobalt ferrite nanoparticles: Preparation, characterization and anionic dye removal capability, " *Journal of The Taiwan Institute of Chemical Engineers*, vol. 59, p. 320–329, 2016.
- [28] R. Sagayaraj, S. Aravazhi, C. S. kumar, S. S. kumar, and G. Chandrasekaran, "Tuning of ferrites (Co_xFe_{3-x}O₄) nanoparticles by co-precipitation technique," *SN Applied Sciences*, vol. 1, p. 1-11, 2019.
- [29] M. Sajjia, M. Oubaha, M. Hasanuzzaman, and A. G. Olabi, "Developments of cobalt ferrite nanoparticles prepared by the sol–gel process," *Ceramics International*, vol. 40, p. 1147–1154, 2014.
- [30] D. Ravinder, M. Hashim, A. Upadhyay, M. M. Ismail, S. Kumar, R. Kumar, *et al.*, "Investigation of structural and magnetic properties of La doped Co–Mn ferrite nanoparticles in the presence of α -Fe₂O₃ phase," *Solid State Communications*, vol. 342, p. 114629–114629, 2022.
- [31] Z. Shaterabadi, G. Nabiyouni, and M. Soleymani, "Physics responsible for heating efficiency and self-controlled temperature rise of magnetic nanoparticles in magnetic hyperthermia therapy," *Progress in Biophysics and Molecular Biology*, vol. 133, p. 9–19, 2018.
- [32] P. Puspitasari and L.S. Budi, "Physical and Magnetic Properties Comparison of Cobalt Ferrite Nanopowder Using Sol-gel and Sonochemical Methods," *International Journal of Engineering*, vol. 33, p. 877-884, 2020.